JOURNAL OF AGRICULTURAL AND FOOD CHEMISTRY

Article

pubs.acs.org/JAFC

Encapsulation of the Herbicide Picloram by Using Polyelectrolyte Biopolymers as Layer-by-Layer Materials

Xiaojing Wang and Jing Zhao*

College of Materials Science and Engineering, Beijing University of Chemical Technology, 15 Beisanhuan East Road, Chao Yang District, Beijing 100029, China

ABSTRACT: Microcapsules of the herbicide picloram (PLR) were formulated by a layer-by-layer (LbL) self-assembly method using the polyelectrolyte biopolymers of biocompatible chitosan (CS) and the UV-absorbent sodium lignosulfonate (SL) as shell materials. The herbicide PLR was recrystallized and characterized using XRD analysis. The obtained PLR-loaded microcapsules were characterized by using SEM, FTIR, CLSM, and ζ-potential measurements. The herbicide loading and encapsulation efficiency were also analyzed for the PLR-loaded microcapsules. The influence of LbL layer numbers on herbicide release and photodegradation rates was investigated in vitro. The results showed that the release rates and photodegradation rates of PLR in microcapsules decreased with increasing number of CS/SL self-assembly layers. The results demonstrated that polyelectrolyte biopolymer-based LbL multilayer microcapsules can be a promising approach for the controlled release of PLR as well as other pesticides with poor photostability or short half-release time.

KEYWORDS: *layer-by-layer, self-assembly, picloram, encapsulation, chitosan, sodium lignosulfonate*

INTRODUCTION

Despite the great effort made by the agrochemical industry in recent years to produce new types of formulations such as suspension concentrate (SC), emulsifiable concentrate (EC), and aqueous solution (AS), there are still important problems derived from the immediate release of the active ingredients, which lead to toxicity risks near the plants as a result of high pesticide concentrations in a short period. Therefore, excessive quantities of these chemical substances are needed to compensate such losses, also resulting in an important economic loss; at the same time, it is harmful to human health as well as the environment.[1] The use of controlled release formulations of pesticides, which are well-known to have many advantages over conventional formulations, particularly for reducing active ingredient release rate and prolonging time of activity, could be a potential solution to the problems mentioned above.[2−4] In controlled release systems, microencapsulation is a versatile technology in which liposomes, microgels, microemulsions, and colloids have been widely employed as pesticide carriers. Many achievements have been made in the field of herbicide encapsulation for controlled release.[5−9]

In recent years, a novel microencapsulation technology based on layer-by-layer (LbL) assembly of oppositely charged polyelectrolytes has been developed.[10−12] With the LbL technique, polyelectrolyte multilayers can be fabricated on various colloid templates such as polymeric particles, organic/inorganic crystals, and blood cells[13,14] due to the electrostatic attraction between oppositely charged polyelectrolytes.[15] Various natural and synthetic polyelectrolytes have been used to constitute the core−shell microcapsules, allowing the capsule wall to be tailored in the nanometer scale.[16] The multilayer films can also be modified with lipids, magnetite nanoparticles, and bioactive immunoglobulin to add special functions to the microcapsules.[17,18] The thickness of the microcapsule wall, which directly influences the core's permeability when diffusing outward and further determines the release rate as well, can be easily tailored by polyelectrolytes species, layer numbers, solution conditions, etc.[19] The LbL assembly technique has become a promising approach and been well documented for microencapsulation in modern medication and pharmaceuticals.[20−23] However, no study on pesticide encapsulated via LbL for controlled release has been reported before. In our work, the herbicide picloram (PLR, Figure 1a) was investigated as the model drug, on which the LbL assembly process was conducted.

Picloram (4-amino-3,5,6-trichloropicolinic acid) (PLR), a chlorinated herbicide, was introduced in 1963 and widely used for controlling annual and perennial shrubs, woody plants, and broadleaf weeds in pasture and cereal crop fields.[24,25] It could be readily absorbed by plants and stimulate DNA, RNA, and protein synthesis at low concentrations but inhibit cell division and growth at higher concentrations.[26] The herbicide is highly active at low application rate[25] but has relatively low toxicity to animal species.[27] However, PLR is relatively water-soluble (430 μg/mL)[28] and easily leaches into surface water and groundwaters, resulting in a risk of groundwater contamination and imposing adverse health and environmental effects.[29−32] On the other hand, PLR is susceptible to rapid photodegradation in water and plant surfaces and has an average half-life of 2.6 days only,[33] which largely restricts its utilization and spraying efficiency. Therefore, it is necessary to investigate a new approach to improving PLR's photostability and actual efficacy and diminish the environmental pollution associated with its application as well.

Received: January 30, 2013
Revised: March 24, 2013
Accepted: April 1, 2013
Published: April 1, 2013

dx.doi.org/10.1021/jf4004658 | J. Agric. Food Chem. 2013, 61, 3789−3796

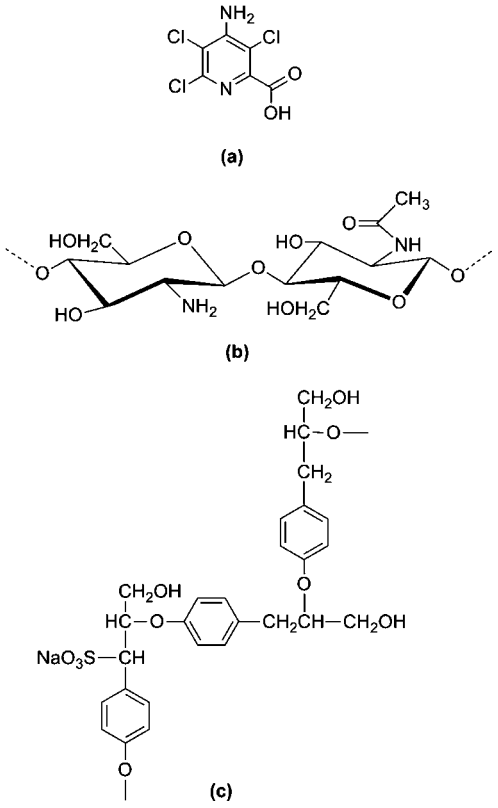

Figure 1. Chemical structures of picloram (a), chitosan (b), and sodium lignosulfonate (c). (In lignosulfonates the relative contents of phenylpropanoid monomers, sulfonate groups, and linkage types are known, but their relative locations as well as the detailed branching pattern and position of charged groups are less well understood. The fragment shown is meant to illustrate general features rather than specifically identified structures.)

In this study, we intended to investigate the controlled release of PLR encapsulated with natural polyelectrolytes chitosan (CS, Figure 1b) and sodium lignosulfonate (SL, Figure 1c) as deposited materials. Natural polyelectrolytes such as chitosan, ethylcellulose, carboxymethocel, lignin, and alginate are preferred to synthetic polymers because of their nontoxicity, biodegradability, low cost, and free availability.[34−37] Chitosan has attracted considerable attention because of its potential wide range of industrial applications and been investigated and used for encapsulation in recent years.[38−41] Noticeably, chitosan is not just a natural antimicrobial in agriculture; its derivatives can also enrich the soil and then increase crop production.[42] Lignosulfonate, a polyanion with sulfonated groups, is a water-soluble and inexpensive product separated from brown liquor by the pulp and paper industries.[43] Its protective properties, such as being UV-light absorbent, an antioxidant, and biodegradable in the environment, make it appropriate for LbL assembly.[44−46] In this study, the picloram microcrystals were used as the LbL template, whereas CS and SL were directly deposited on the template alternately. The morphology, encapsulation efficiency, and herbicide loading as well as the photostability of PLR-loaded microcapsules were investigated. The release characteristics of those PLR-loaded (CS/SL) microcapsules were investigated in vitro related to the layer numbers of self-assembly and the fine structure of the microcapsules. The results gained would provide further understanding of the remarkable controlled release characteristics of polyelectrolyte biopolymer used as layer-by-layer materials.

MATERIALS AND METHODS

Materials. Commercial PLR was provided by Lier Chemical Co., Ltd., China. Chitosan (deacetylation, 95%; average M_w, 532000 g/mol; viscosity, 80−90 cps; AK Biotech Ltd., China) and sodium lignosulfonate (technical grade, average M_w, 5300 g/mol; sulfonic group content, 1.15 mmol/g; Huaweiyoubang Co., Ltd., China) were selected as polyelectrolytes for the LbL assembly. Sodium dodecyl benzene sulfonate (SDBS) was purchased from Sinopharm Chemical Reagent Co., Ltd., China, and fluorescein isothiocyanate (FITC) from Sigma. Other chemicals were all analytical reagents and used as received. The water used throughout the experiments was purified by a Hi-tech Master-Q purification system and had a resistivity of >18.2 MΩ·cm.

Recrystallization. The picloram powder was dissolved into sodium hydroxide solution (1 mol/L, 50 °C) under rapid agitation, and then, with the presence of SDBS (0.2 g/L), an excess amount of hydrochloric acid (1 mol/L, 50 °C) was added under stirring until the pH value of the solution reduced to approximately 1. The mixture was precipitated for several hours and then filtered with the nylon membrane filters. Finally, the recrystallized microcrystals obtained were dried in air and kept in a desiccator for further use. All operations were performed in the dark.

Encapsulation of PLR Microcrystals by LbL Assembly. The encapsulation process of PLR microcrystals by LbL assembly is shown in Figure 2. To prevent the PLR microcrystals from dissolving during the LbL assembly procedure, the rinsing water used during the experiment was saturated with PLR. The CS solution was prepared by dissolving CS powder into acetic acid solution (2%, v/v) by gentle stirring. The ionic strength was adjusted to 0.5 M by adding NaCl, and the pH value was adjusted to 4 using sodium hydroxide solution. Only freshly prepared CS solution (<8 h) was used throughout the experiment. The SL solution was prepared by dissolving SL powder into deionized water. The ionic strength was also adjusted to 0.5 M by adding NaCl, and the pH value was adjusted to 4 by adding acetic acid solution. For the deposition of the first layer onto the PLR microcrystals, the positively charged CS solution (2 mg/mL, 1 mL) was added into the acetic acid solution of PLR microcrystals (50 mg) with a pH of 4. After being gently shaken (15 min), the suspension was centrifuged using a centrifuge (TGL-16G, Shanghai, China) at 10000 rpm for 5 min. The supernatant was discarded. The CS-coated microcrystals were thoroughly washed with PLR-saturated solution twice to remove the excess polyelectrolyte before further assembly. For the following deposition of SL layer onto the CS-coated microcrystals, the negatively charged SL solution (2 mg/mL, 1 mL) was added into the acetic acid solution of the CS-coated PLR microcrystals (50 mg) with a pH of 4. Consecutive alternating CS and SL layers were deposited until the desired layers of coating was achieved.

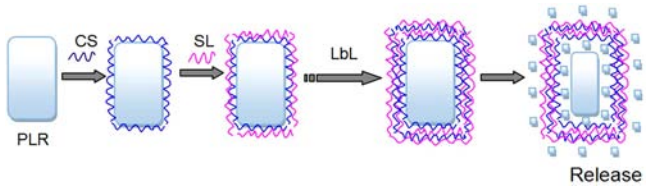

Figure 2. Illustration of the encapsulation of PLR microcrystals by LbL assembly and drug release from the PLR microcapsules. (This schematic drawing is to demonstrate the LbL self-assembly process rather than the actual size of the wall and core in the microcapsules.)

Measurements of the Herbicide Loading (HL) and Encapsulation Efficiency (EE). To determine the HL, accurately weighed 10 mg microcapsules were added into ethanol and PLR was thoroughly dissolved in ethanol. The UV absorbance of PLR concentration in ethanol was determined on a TU-1810 UV−vis

dx.doi.org/10.1021/jf4004658 | J. Agric. Food Chem. 2013, 61, 3789−3796

spectrophotometer at 224 nm, and then the HL and EE were calculated according to eqs 1 and 2, respectively.

$$\text{HL}\ (\%) = \frac{\text{mass of herbicide in microcapsules}}{\text{mass of microcapsules}} \times 100 \quad (1)$$

$$\text{EE}\ (\%) = \frac{\text{mass of herbicide in microcapsules}}{\text{initial mass of herbicide}} \times 100 \quad (2)$$

Measurement of Herbicide Release. Picloram release from the PLR-loaded CS/SL microcapsules (10 mg) was investigated in vitro at 25 °C in 300 mL reagent bottles containing 200 mL of an ethanol−water solution (5%, v/v) using a controlled environment incubator orbital shaker (Tianyou Co., Jiangsu Province, China) at 150 rpm. After different time intervals, 1 mL of solution was sampled and 1 mL of fresh ethanol−water solution was added to the reagent bottle to maintain constant volume and "sink" condition. The sampled solution was then filtered through a cellulose membrane filter (diameter,13 mm; pore size, 0.45 μm; Membrance Solutions Inc.) prior to UV analysis and was analyzed on a TU-1810 UV−vis spectrophotometer at 224 nm for determination of PLR released. The amount of PLR released was calculated by UV absorbance measured with the help of the calibration curve of PLR (0.5−18 mg/L).[47] The same experiment was done with the uncoated PLR as a control for comparison. All release experiments were conducted in triplicates at room temperature (~25 °C).

Photodegradation Measurement. Accurately weighed microcapsules (each sample contained an equivalent amount of the active ingredient PLR of 10 mg) coated with 4, 8, and 12 layers together with uncoated PLR as a control were dispersed in PLR saturated solution for investigation of the photostability of PLR. Samples in transparent glass vessels were placed in a light-proof cabinet and exposed to UV light for up to 30 min. A 103 W mercury short arc lamp ($\lambda = 365 \pm 15$ nm) was used as the exciting light source for UV irradiation. The intensity of light was controlled to be ~5 mW/cm^2. After certain time intervals, 0.5 mL of sample was collected from each treatment, and then PLR was extracted with ethanol and measured by UV analysis.

Scanning Electron Microscopy (SEM). The morphologies of PLR microcrystals before and after recrystallization as well as the feature of hollow capsules collected at the end of the release experiment were characterized by SEM (Hitachi S-4700, Japan, operated at 20 kV). The sample suspension was dropped onto a glass slide, dried in air, and then sputtered with gold before observation.

Confocal Laser Scanning Microscopy (CLSM). To validate the distribution of depositing materials on the microcrystals, FITC was used to label the chitosan to make the microcapsules visualized.[48] The coated picloram microcrystals were observed under a FV1000-IX81 confocal scanning system (Olympus) equipped with a 100× oil immersion objective with a numerical aperture (NA) of 1.4, and the excitation wavelength was 488 nm.

XRD Measurement. Powder X-ray diffraction patterns were measured by a diffractometer (UTtima III, Japan) using Cu Kα radiation. The samples were analyzed for 2θ values from 5 to 70 with a scanning speed of 5°/min.

ζ-Potential Measurement. The charges on the PLR microcrystal surface after the deposition of consecutive polyelectrolyte layers were monitored using a zeta-sizer (Zetaplus, USA). The coated PLR microparticles were redispersed in deionized water, and the ζ-potential was determined from their mobility measurement. For each sample, six successive measurements were carried out to get an average.

FTIR Spectra. Infrared spectra of all samples were performed using KBr pellets in the 4000−400 cm^{-1} region using a Nicolet 380 spectrophotometer.

RESULTS AND DISCUSSION

Recrystallization. The release rates of the drug from microcapsules were affected by internal factors such as the species and properties of shell materials, the shape and size of the drug as well as its solubility, and some external conditions (pH, ionic strength, etc.) employed.[22] The commercial PLR microcrystals have irregular shape and rough surface and are different in size, as shown in Figure 3a, which poses an adverse

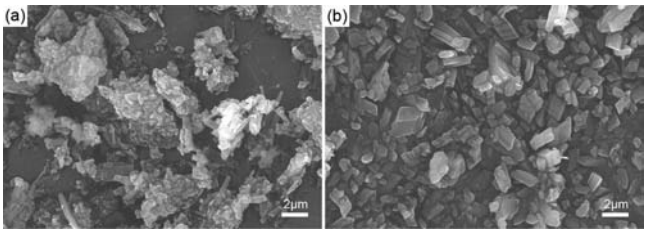

Figure 3. SEM micrographs of PLR microcrystals before (a) and after (b) recrystallization.

effect on the further assembly of polyelectrolytes onto the microcrystals. Especially, the microcrystals with different size would dissolve at different speeds according to their surface-to-volume ratio, which exerts an influence directly upon the herbicide release rates and is disadvantageous to the subsequent investigation of the release mechanism of PLR from microcapsules. Thus, it is necessary to implement a recrystallization process of PLR for homogeneous microcrystals. PLR is an acidic herbicide in the pyridine carboxylic acid family, and its solubility is expected to decrease as pH decreases; the commercial PLR powders were thus dissolved thoroughly in alkaline solution and recrystallized by adjusting the pH close to 1.[49] The morphology of the obtained microcrystals is shown in Figure 3b. In comparison with the commercial PLR, the recrystallized microcrystals are in a columnar shape with approximately uniform length of about 1−4 μm. The obtained microcrystals with regular shape and similar size are beneficial for the further encapsulation by self-assembly and the in vitro release study. The results are in accordance with the conclusion from X-ray diffraction of the PLR before and after recrystallization. As shown in Figure 4, both patterns exhibited

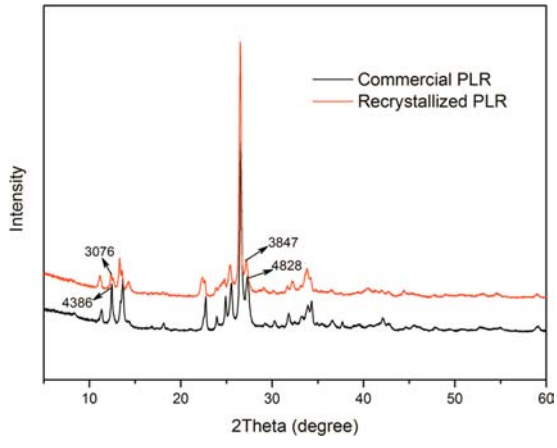

Figure 4. X-ray diffraction patterns of PLR before and after recrystallization.

a strong diffraction peak at a 2θ value of 26, indicating its crystal structure. In contrast to the commercial PLR, the characteristic peak of the microcrystals obtained from recrystallization is much stronger, with a few other peaks weakened in intensity. The XRD data demonstrate that the recrystallized microcrystals possess a higher orientation degree as the result of a realignment process, forming more regular structure.

dx.doi.org/10.1021/jf4004658 | J. Agric. Food Chem. 2013, 61, 3789−3796

Encapsulation of PLR Microcrystals. The alternative deposition of CS and SL onto the PLR microcrystals was monitored by ζ-potential measurement with the results shown in Figure 5. The uncoated microcrystal surface was negatively

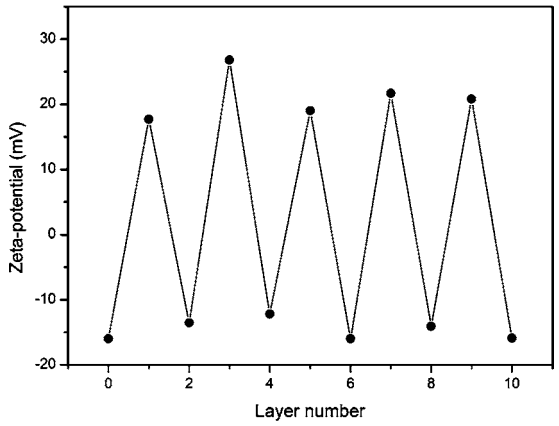

Figure 5. ζ-Potential on the surface of the PLR-loaded microcapsules with different layer numbers of self-assembly.

charged with a potential of −16 mV, serving as the substrate for the adsorption of CS polycation as the first layer. The potential was converted to +18 mV for the first layer CS and around −14 mV for the first layer SL and then changed alternatively afterward. The surface-modified microcrystals were prevented from aggregating because of the ionic and/or steric interactions of the thin coating and, thus, stable in the aqueous solution. The obvious alternative changes in the surface charges between opposite signs were strong evidence that the alternating deposition of CS and SL onto the microcrystals was achieved, which was also the characteristic of the polyelectrolyte multilayer formulation via the LbL assembly process.[41]

The SEM images of PLR microcrystals before and after coating are shown in Figure 6. By comparison of the insets shown in Figure 6a,b, it is obvious that the uncoated microcrystals had a smooth surface, whereas the microcrystals encapsulated with five bilayers of CS/SL had a much rougher

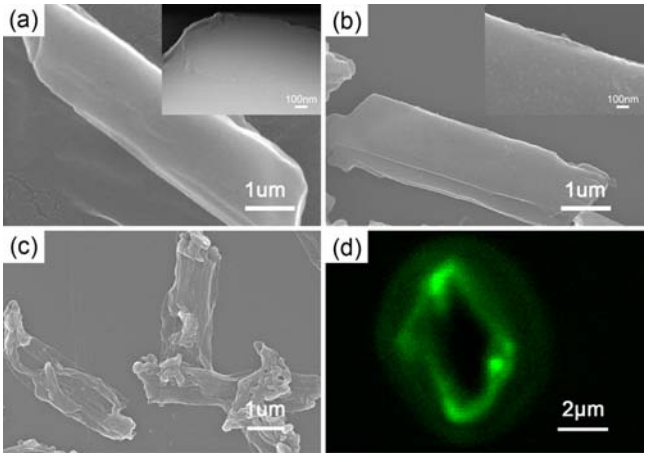

Figure 6. SEM micrographs of (a) the recrystallized PLR microcrystals and (b) PLR microcrystals after coating with five bilayers (insets are closeups of their corresponding surfaces); (c) hollow microcapsules after complete release of PLR; (d) CLSM image of PLR microcrystals coated with five bilayers of FITC-CS/SL.

surface. This result can be explained by the formation of a polyelectrolyte film onto the microcrystal surface, and the polyelectrolyte film shrunk when dried for SEM measurement. Figure 6c depicts the image of the hollow microcapsules collected at the end of the release experiment, in which the collapsed structure with its integrity maintained is clearly demonstrated. The folds and ruffles on the surface of the microcapsules are rather typical for collapsed hollow microcapsules due to water evaporation during drying and the removal of drug from the inside.[50] CLSM was also employed to verify the coating on PLR microcrystals with polyelectrolyte multilayers. The homogeneous green fluorescence intensity suggests a uniform polyelectrolyte distribution due to the effective probing of FITC to chitosan. All of the aforementioned results plus the alternative reverse of the colloid surface charge demonstrated that the fabrication of polyelectrolyte multilayers onto PLR microcrystals via LbL self-assembly was successful.

However, there was an inevitable loss of PLR microcrystals as a result of frequent centrifugation and a rinse step during the self-assembly procedure. It was anticipated that some of the microcrystals would partially dissolve in the solutions of rinse and redispersal, as well as adhere to the container walls in the rinsing process. The encapsulation efficiency calculated on the basis of UV absorbance of the extracts collected from the ethanol solution of PLR microcapsules decreased from 87.6% for the PLR microcapsules with four layers to 72.7% for the microcapsules with eight layers and even further to 49.8% for the microcapsules with 12 layers. Therefore, high retention for the drug encapsulation via the LbL self-assembly process is still an open question in the technology.[20]

FTIR spectra of CS, SL, PLR microcrystals, PLR-loaded microcapsules with $(CS/SL)_5$, and the CS/SL shell after thorough extraction of PLR microcrystals are shown in Figure 7. For CS, the absorption band located at 3424 cm^{-1} originates

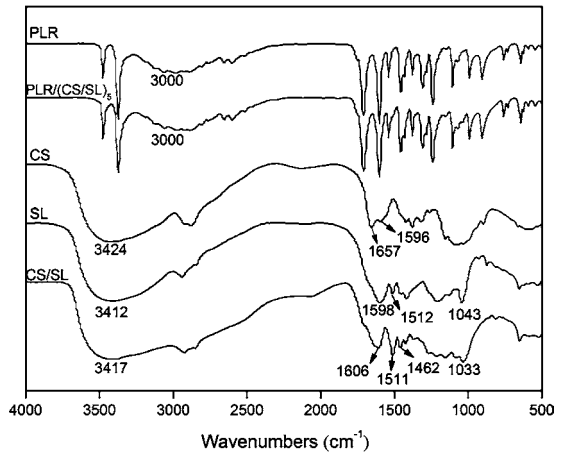

Figure 7. FTIR spectra of CS, SL, PLR microcrystals, PLR/$(CS/SL)_5$ microcapsules, and CS/SL shell after complete release of PLR.

from the stretching vibration of the N−H group combined with the O−H group, and the peaks at 1657 and 1596 cm^{-1} are ascribed to amide I and II bands.[51,52] As to SL, the absorption bands at 1512 and 1043 cm^{-1} are attributed to the C_9 aromatic skeletal vibration and the stretching vibration of the S═O, respectively. For the CS/SL shell, the original characteristic absorptions of S═O group at 1043 cm^{-1} for SL and the amide I, II at 1657 and 1596 cm^{-1} for CS almost disappear, whereas

new absorption peaks appear at 1606 and 1462 cm^{-1}, which indicates strong electrostatic interaction between negatively charged sulfuric acid ions ($-SO_3^-$) on SL and the positively charged amino groups ($-NH_3^+$) on CS. Moreover, the characteristic absorption of PLR microcrystals can hardly be detected in the spectrum of CS/SL shell, indicating the complete dissolution of the microcrystal cores. With respect to the PLR microcrystals, the spectra before and after coating are nearly identical, which demonstrates well the chemical structure of PLR was not changed during the whole LbL assembly procedure. The herbicide loading of PLR-loaded microcapsules (shown in Table1) also suggests that the amount of polyelectrolyte shell is low in the entire microcapsule.

Table 1. Characteristic Parameters of PLR-Loaded Microcapsules

layer	HL[a] (%)	EE[b] (%)	$K \times 10^{-2}$ (h^{-n})	n[c]	r[d]	t_{50}[e] (h)
4	96.7	87.6	64.85	0.311 ± 0.053	0.947	0.433
8	95.2	72.7	49.66	0.453 ± 0.020	0.993	1.015
12	93.3	49.8	32.53	0.528 ± 0.018	0.994	2.257

[a]The herbicide loading of the PLR-loaded microcapsules. [b]The encapsulation efficiency of the PLR-loaded microcapsules. [c]The diffusion parameter for the release mechanism. [d]Correlation coefficient. [e]The time required for 50% release of PLR.

Photostability of PLR-Loaded Microcapsules. The remaining PLR in microcapsules obtained from the photostability measurement are displayed in Figure 8 as a function of reaction time. The control sample (uncoated PLR) underwent a rapid photodegradation, with only about 30% of PLR remaining after UV exposure for 10 min. By contrast, the degradation rates of all PLR-loaded microcapsules appeared to reduce remarkably, with >50% of PLR remaining in samples after being exposed to UV light irradiation for 30 min. Furthermore, the amount of PLR remaining in microcapsules increased as the layer numbers increased. The improvement in photostability of PLR was owing to sodium lignosulfonate, which could absorb UV light and was used as the anionic polyelectrolyte of LbL assembly material for encapsulation of PLR, providing great protection for the PLR core against UV light-induced degradation. On the other hand, the use of chitosan as the cationic polyelectrolyte of LbL assembly material for encapsulation of PLR can also provide protection for the PLR core, leading to reduction in the photodegradation of PLR.

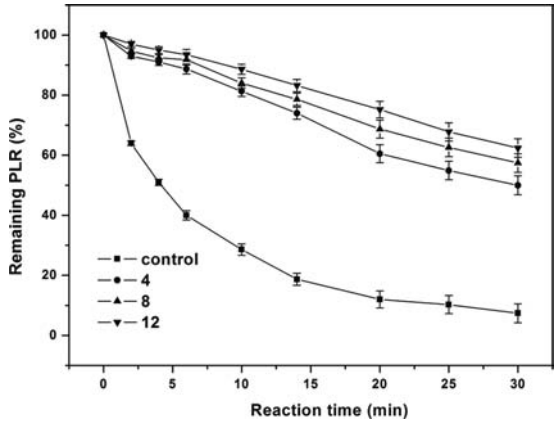

Figure 8. Percentage of PLR remaining in microcapsules with 4, 8, and 12 layers after being exposed to UV light for 30 min in comparison to the uncoated PLR as a control (error bars represent the standard deviation of three replicates).

In Vitro Release Experiment. The amount of PLR released from microcapsules with different polyelectrolyte layers was quantified by measuring the UV absorbance of the sample collected at different time intervals from the solution containing the PLR-loaded microcapsules. These data are shown as a function of time in Figure 9 together with that of the uncoated PLR for comparison. The half release times t_{50} (shown in Table 1) were 0.43, 1.02, and 2.26 h for the PLR-loaded microcapsules with 4, 8, and 12 polyelectrolyte layers, respectively, compared with 0.05 h for the uncoated PLR microcrystals. Thus, the t_{50} values were 9, 20, and 45 times longer for the PLR-loaded microcapsules than for the uncoated PLR. The total release times for the corresponding microcapsules were 4.66, 7.28, and 10.75 h, whereas the uncoated PLR microcrystals dissolved completely in 4.18 h. It seems that the PLR microcrystals encapsulated with 4 layers of polyelectrolytes make no significant difference to the total release time, whereas the 8 and 12 layer coatings of polyelectrolytes were thick enough to provide much slower release. As expected, the release rates of PLR from the PLR-loaded microcapsules decreased as the layer number of the microcapsules increased. Similar results have been observed for encapsulation and release of several biomedicines such as ibuprofen, indomethacin, furosemide, and camptothecin.[20−22,53] This decrease in the multilayer permeability was attributed to the increase in shell thickness and partial closure of the pores existing in the deposited polyelectrolyte layers with further deposition.

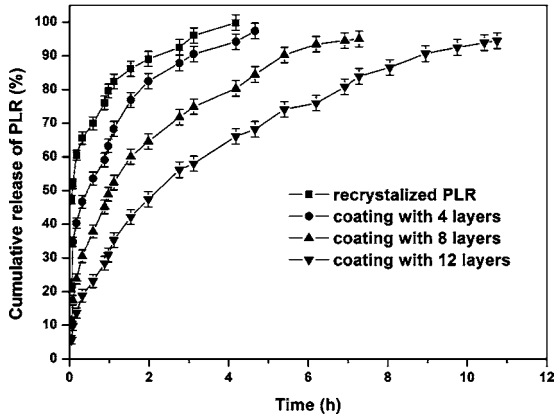

Figure 9. Release profiles of PLR from (CS/CL) microcapsules with 0, 4, 8, and 12 polyelectrolyte layers (error bars represent the standard deviation of three replicates).

In a controlled release system, a major problem is the obvious initial burst during which a great amount of drug releases, resulting in an acutely high drug concentration and failure of the controlled release.[54,55] As we can see from Figure 9, there was an initial burst in the release profile of the uncoated PLR microcrystals, whereas that of PLR from microcapsules appeared to be depressed considerably during the whole process. Furthermore, the initial burst of the microcapsules with 12 layers lasted for the shortest time among the samples. These results demonstrate that the multilayer encapsulation of the PLR microcrystals can not only prolong the release time but

also depress the initial "burst effect" to some degree. Therefore, it should be possible to design controlled-release microdevices with desirable release rates by regulating the deposited polyelectrolyte layers during the LbL assembly process.

Finally, the release mechanisms of the PLR were also investigated for the CS/SL microcapsules. The release of PLR from the CS/SL microcapsules should involve two courses: (i) the bulk solution diffuses into the microcapsules to dissolve the core microcrystals, and (ii) the dissolved PLR molecules diffuse out of the microcapsules. It is expected that at the early release stage the PLR concentration within the microcapsules is very high (≈ its saturation concentration), and the same concentration is sustained until the core microcrystals dissolve completely.[56] During this period, the permeability of the microcapsule shell is the determining factor controlling the release rates, explaining why the release rate decreases as the microcapsule wall thickness increases.[22] Here, we analyzed the kinetic release data of the PLR from microcapsules by applying the empirical equation[57]

$$M_t/M_0 = Kt^n \quad (3)$$

where M_t/M_0 is the percentage of active ingredient released at time t, K is a constant that incorporates characteristics of the macromolecular network system and the active ingredient, and n is a diffusional parameter, which is indicative of the transport mechanism.

The values of K, n, and t_{50} obtained from the initial 60% of PLR released are presented in Table 1. According to correlation coefficients, we can deduce that the release profiles of PLR from microcapsules with 8 and 12 layers fit well to the empirical equation. The values of the parameter n for 8 and 12 layer capsules are 0.453 and 0.528, which are very close to 0.5 reported for the diffusion mechanism of spherical formulations in the ref 57. The results suggested that the release mechanism of PLR from the (CS/CL) microcapsules in this study is Fickian diffusion.

In summary, recrystallized PLR microcrystals have been successfully encapsulated by a layer-by-layer self-assembly method using polyelectrolyte biopolymers of chitosan and sodium lignosulfonate as the mutilayer wall materials. Improved photostability and sustained drug release were achieved for the PLR-loaded (CS/CL) microcapsules. Both the photodegradation and release rates of PLR from (CS/CL) microcapsules decreased as the layer numbers of self-assembly increased. The results suggest that the polyelectrolyte biopolymers can be used as assembly materials for encapsulation of low water-soluble pesticide for controlled release. There are some limitations of the LbL assembly process for pesticide encapsulation at the current stage, such as restricted applicability to ionizable pesticides as model compounds only, low encapsulation efficiency, and high cost to achieve multiple-layer encapsulations. Nevertheless, the LbL self-assembly method for the encapsulation of pesticides is a promising method for the precisely controlled release of herbicides and has potential practical applications. Additionally, the use of sodium lignosulfonate as the wall material for encapsulation of pesticides could be a new approach for applying the low-cost SL in the controlled release of pesticides. An approach for further increasing the EE and simplifying the self-assembly process needd further study.

AUTHOR INFORMATION

Corresponding Author

*Phone: 010-64453362. Fax: 010-64414824. E-mail: zhaojing@mail.buct.edu.cn.

Funding

We acknowledge the National Natural Science Foundation of China (No. 51073018) for financial support.

Notes

The authors declare no competing financial interest.

ABBREVIATIONS USED

CS, chitosan; CLSM, confocal laser scanning microscopy; EE, encapsulation efficiency; FITC, fluorescein isothiocyanate; FTIR, Fourier transform infrared spectroscopy; HL, herbicide loading; LbL, layer-by-layer; PLR, picloram; SL, sodium lignosulfonate; SEM, scanning electron microscopy; SDBS, sodium dodecyl benzene sulfonate; XRD, X-ray diffraction

REFERENCES

(1) Flores-Cespedes, F.; Fernandez-Perez, M.; Villafranca-Sanchez, M.; Gonzalez-Pradas, E. Cosorption study of organic pollutants and dissolved organic matter in a soil. *Environ. Pollut. (Amsterdam, Netherlands)* **2006**, *142*, 449−456.

(2) Akelah, A. Novel utilizations of conventional agrochemicals by controlled release formulations. *Mater. Sci. Eng., C: Biomimetic Mater., Sensors Syst.* **1996**, *C4*, 83−98.

(3) Rudzinski, W. E.; Dave, A. M.; Vaishnav, U. H.; Kumbar, S. G.; Kulkarni, A. R.; Aminabhavi, T. M. Hydrogels as controlled release devices in agriculture. *Des. Monomers Polym.* **2002**, *5*, 39−65.

(4) Gerstl, Z.; Nasser, A.; Mingelgrin, U. Controlled release of pesticides into soils from clay-polymer formulations. *J. Agric. Food Chem.* **1998**, *46*, 3797−3802.

(5) Grillo, R.; Pereira Ado, E.; de Melo, N. F.; Porto, R. M.; Feitosa, L. O.; Tonello, P. S.; Dias Filho, N. L.; Rosa, A. H.; Lima, R.; Fraceto, L. F. Controlled release system for ametryn using polymer microspheres: preparation, characterization and release kinetics in water. *J. Hazard. Mater.* **2011**, *186*, 1645−1651.

(6) Fernández-Pérez, M.; Villafranca-Sánchez, M.; Flores-Céspedes, F.; Daza-Fernández, I. Ethylcellulose and lignin as bearer polymers in controlled release formulations of chloridazon. *Carbohydr. Polym.* **2011**, *83*, 1672−1679.

(7) Flores Cespedes, F.; Villafranca Sanchez, M.; Perez Garcia, S.; Fernandez Perez, M. Modifying sorbents in controlled release formulations to prevent herbicides pollution. *Chemosphere* **2007**, *69*, 785−794.

(8) Elbahri, Z.; Taverdet, J. L. Optimization of an herbicide release from ethylcellulose microspheres. *Polym. Bull. (Heidelberg, Germany)* **2005**, *54*, 353−363.

(9) Zhu, Z.; Zhuo, R. Slow release behavior of starch-g-poly(vinyl alcohol) matrix for 2,4,5-trichlorophenoxyacetic acid herbicide. *Eur. Polym. J.* **2001**, *37*, 1913−1919.

(10) Gao, C.; Donath, E.; Mohwald, H.; Shen, J. Spontaneous deposition of water-soluble substances into microcapsules. Phenomenon, mechanism, and application. *Angew. Chem., Int. Ed.* **2002**, *41*, 3789−3793.

(11) Sukhorukov, G. B.; Donath, E.; Lichtenfeld, H.; Knippel, E.; Knippel, M.; Budde, A.; Mohwald, H. Layer-by-layer self assembly of polyelectrolytes on colloidal particles. *Colloids Surf., A: Physicochem. Eng. Aspects* **1998**, *137*, 253−266.

(12) Daehne, L.; Leporatti, S.; Donath, E.; Moehwald, H. Fabrication of micro reaction cages with tailored properties. *J. Am. Chem. Soc.* **2001**, *123*, 5431−5436.

(13) Leporatti, S.; Voigt, A.; Mitloehner, R.; Sukhorukov, G.; Donath, E.; Moehwald, H. Scanning force microscopy investigation of polyelectrolyte nano- and microcapsule wall texture. *Langmuir* **2000**, *16*, 4059−4063.

(14) Moya, S.; Sukhorukov, G. B.; Auch, M.; Donath, E.; Mohwald, H. Microencapsulation of organic solvents in polyelectrolyte multilayer micrometer-sized shells. *J. Colloid Interface Sci.* **1999**, *216*, 297−302.
(15) Donath, E.; Sukhorukov, G. B.; Caruso, F.; Davis, S. A.; Mohwald, H. Novel hollow polymer shells by colloid-templated assembly of polyelectrolytes. *Angew. Chem., Int. Ed.* **1998**, *37*, 2202−2205.
(16) Gao, C.; Leporatti, S.; Donath, E.; Moehwald, H. Surface texture of poly(styrenesulfonate sodium salt) and poly-(diallyldimethylammonium chloride) micron-sized multilayer capsules: a scanning force and confocal microscopy study. *J. Phys. Chem. B* **2000**, *104*, 7144−7149.
(17) Moya, S.; Donath, E.; Sukhorukov, G. B.; Auch, M.; Baeumler, H.; Lichtenfeld, H.; Moehwald, H. Lipid coating on polyelectrolyte surface modified colloidal particles and polyelectrolyte capsules. *Macromolecules* **2000**, *33*, 4538−4544.
(18) Voigt, A.; Lichtenfeld, H.; Sukhorukov, G. B.; Zastrow, H.; Donath, E.; Baeumler, H.; Moehwald, H. Membrane filtration for microencapsulation and microcapsules fabrication by layer-by-layer polyelectrolyte adsorption. *Ind. Eng. Chem. Res.* **1999**, *38*, 4037−4043.
(19) Sukhorukov, G. B.; Donath, E.; Moya, S.; Susha, A. S.; Voigt, A.; Hartmann, J.; Mohwald, H. Microencapsulation by means of step-wise adsorption of polyelectrolytes. *J. Microencapsulation* **2000**, *17*, 177−185.
(20) Ye, S.; Wang, C.; Liu, X.; Tong, Z. Deposition temperature effect on release rate of indomethacin microcrystals from microcapsules of layer-by-layer assembled chitosan and alginate multilayer films. *J. Controlled Release* **2005**, *106*, 319−328.
(21) Ai, H.; Jones, S. A.; deVilliers, M. M.; Lvov, Y. M. Nano-encapsulation of furosemide microcrystals for controlled drug release. *J. Controlled Release* **2003**, *86*, 59−68.
(22) Qiu, X.; Leporatti, S.; Donath, E.; Moehwald, H. Studies on the drug release properties of polysaccharide multilayers encapsulated ibuprofen microparticles. *Langmuir* **2001**, *17*, 5375−5380.
(23) Caruso, F.; Yang, W.; Trau, D.; Renneberg, R. Micro-encapsulation of uncharged low molecular weight organic materials by polyelectrolyte multilayer self-assembly. *Langmuir* **2000**, *16*, 8932−8936.
(24) Wells, M. J.; Yu, L. Z. Solid-phase extraction of acidic herbicides. *J. Chromatogr., A* **2000**, *885*, 237−250.
(25) Hamaker, J. W.; Johnston, H.; Martin, R. T.; Redemann, C. T. A picolinic acid derivative: a plant growth regulator. *Science* **1963**, *141*, 363.
(26) dos Santos, L. B. O.; Masini, J. C. Determination of picloram in natural waters employing sequential injection square wave voltammetry using the hanging mercury drop electrode. *Talanta* **2007**, *72*, 1023−1029.
(27) Lynn, G. E. Review of toxicological information on Tordon herbicides. *Down to Earth* **1965**, *20*, 6−8.
(28) Herr, D. E.; Stroube, E. W.; Ray, D. A. The movement and persistence of picloram in soil. *Weeds* **1966**, *14*, 248−250.
(29) Fryer, J. D.; Smith, P. D.; Ludwig, J. W. Long-term persistence of picloram in a sandy loam soil. *J. Environ. Qual.* **1979**, *8*, 83−86.
(30) Hance, R. J. Decomposition of herbicides in the soil by nonbiological chemical process. *J. Sci. Food Agric.* **1967**, *18*, 544−547.
(31) Ghauch, A. Degradation of benomyl, picloram, and dicamba in a conical apparatus by zero-valent iron powder. *Chemosphere* **2001**, *43*, 1109−1117.
(32) Tang, L.; Zeng, G.-M.; Shen, G.-L.; Li, Y.-P.; Zhang, Y.; Huang, D.-L. Rapid detection of picloram in agricultural field samples using a disposable immunomembrane-based electrochemical sensor. *Environ. Sci. Technol.* **2008**, *42*, 1207−1212.
(33) Woodburn, K. B.; Fontaine, D. D.; Bjerke, E. L.; Kallos, G. J. Photolysis of picloram in dilute aqueous solution. *Environ. Toxicol. Chem.* **1989**, *8*, 769−775.
(34) Ferreira Almeida, P.; Almeida, A. J. Cross-linked alginate-gelatin beads: a new matrix for controlled release of pindolol. *J. Controlled Release* **2004**, *97*, 431−439.
(35) Sopena, F.; Cabrera, A.; Maqueda, C.; Morillo, E. Controlled release of the herbicide norflurazon into water from ethylcellulose formulations. *J. Agric. Food Chem.* **2005**, *53*, 3540−3547.
(36) Isiklan, N. Controlled release of insecticide carbaryl from sodium alginate, sodium alginate/gelatin, and sodium alginate/sodium carboxymethyl cellulose blend beads crosslinked with glutaraldehyde. *J. Appl. Polym. Sci.* **2006**, *99*, 1310−1319.
(37) Zhao, J.; Wilkins, R. M. Controlled release of the herbicide, fluometuron, from matrix granules based on fractionated organosolv lignins. *J. Agric. Food Chem.* **2003**, *51*, 4023−4028.
(38) Shahidi, F.; Arachchi, J. K. V.; Jeon, Y.-J. Food applications of chitin and chitosans. *Trends Food Sci. Technol.* **1999**, *10*, 37−51.
(39) Han, J.; Guenier, A.-S.; Salmieri, S.; Lacroix, M. Alginate and chitosan functionalization for micronutrient encapsulation. *J. Agric. Food Chem.* **2008**, *56*, 2528−2535.
(40) Luo, Y.; Teng, Z.; Wang, Q. Development of zein nanoparticles coated with carboxymethyl chitosan for encapsulation and controlled release of vitamin D3. *J. Agric. Food Chem.* **2012**, *60*, 836−843.
(41) Priya, A. J.; Vijayalakshmi, S. P.; Raichur, A. M. Enhanced survival of probiotic *Lactobacillus acidophilus* by encapsulation with nanostructured polyelectrolyte layers through layer-by-layer approach. *J. Agric. Food Chem.* **2011**, *59*, 11838−11845.
(42) Harish Prashanth, K. V.; Tharanathan, R. N. Chitin/chitosan: modifications and their unlimited application potential − an overview. *Trends Food Sci. Technol.* **2007**, *18*, 117−131.
(43) Lue, Q.-F.; He, Z.-W.; Zhang, J.-Y.; Lin, Q. Preparation and properties of nitrogen-containing hollow carbon nanospheres by pyrolysis of polyaniline-lignosulfonate composites. *J. Anal. Appl. Pyrolysis* **2011**, *92*, 152−157.
(44) Soms, A.; Shul'ga, G. M.; Telysheva, G. M. Effect of UV radiation on the structure and properties of lignosulfonates. *Koksnes Kimija* **1988**, 61−66.
(45) Kleinert, T. N. The UV-degradation of lignin. *Papier (Bingen, Germany)* **1970**, *24*, 563−566.
(46) Zhao, J.; Wilkins, R. M. Controlled release of a herbicide from matrix granules based on solvent-fractionated organosolv lignins. *J. Agric. Food Chem.* **2000**, *48*, 3651−3661.
(47) Lee, D.-J.; Senseman, S. A.; Sciumbato, A. S.; Jung, S.-C.; Krutz, L. J. The effect of titanium dioxide alumina beads on the photocatalytic degradation of picloram in water. *J. Agric. Food Chem.* **2003**, *51*, 2659−2664.
(48) Huang, M.; Khor, E.; Lim, L.-Y. Uptake and cytotoxicity of chitosan molecules and nanoparticles: effects of molecular weight and degree of deacetylation. *Pharm. Res.* **2004**, *21*, 344−353.
(49) Cheung, M. W.; Biggar, J. W. Solubility and molecular structure of 4-amino-3,5,6-trichloropicolinic acid in relation to pH and temperature. *J. Agric. Food Chem.* **1974**, *22*, 202−206.
(50) Xu, L.; Guo, Y.; Liao, Q.; Zhang, J.; Xu, D. Morphological control of ZnO nanostructures by electrodeposition. *J. Phys. Chem. B* **2005**, *109*, 13519−13522.
(51) Song, Z.; Yin, J.; Luo, K.; Zheng, Y.; Yang, Y.; Li, Q.; Yan, S.; Chen, X. Layer-by-layer buildup of poly(L-glutamic acid)/chitosan film for biologically active coating. *Macromol. Biosci.* **2009**, *9*, 268−278.
(52) Dai, Z.; Yin, J.; Yan, S.; Cao, T.; Ma, J.; Chen, X. Polyelectrolyte complexes based on chitosan and poly(L-glutamic acid). *Polym. Int.* **2007**, *56*, 1122−1127.
(53) Guo, S.; Zheng, J.; Dong, J.; Guo, N.; Jing, L.; Yue, X.; Yan, X.; Wang, Y.; Dai, Z. Iron/dextran sulfate multilayered microcapsules for controlled release of 10-hydroxycamptothecin. *Int. J. Biol. Macromol.* **2011**, *49*, 409−415.
(54) Herzfeldt, C. D.; Kuemmel, R. Dissociation constants, solubilities and dissolution rates of some selected nonsteroidal antiinflammatories. *Drug Dev. Ind. Pharm.* **1983**, *9*, 767−793.
(55) Vayssieres, L.; Chaneac, C.; Tronc, E.; Jolivet, J. P. Size tailoring of magnetite particles formed by aqueous precipitation: an example of thermodynamic stability of nanometric oxide particles. *J. Colloid Interface Sci.* **1998**, *205*, 205−212.

(56) Antipov, A. A.; Sukhorukov, G. B.; Donath, E.; Moehwald, H. Sustained release properties of polyelectrolyte multilayer capsules. *J. Phys. Chem. B* **2001**, *105*, 2281−2284.
(57) Ritger, P. L.; Peppas, N. A. A simple equation for description of solute release. I. Fickian and non-Fickian release from non-swellable devices in the form of slabs, spheres, cylinders or disks. *J. Controlled Release* **1987**, *5*, 23−36.